Interrelations between the Mesomeric and Electronegativity Effects in *Para*-Substituted Derivatives of Phenol/Phenolate and Aniline/Anilide H-Bonded Complexes: A DFT-Based Computational Study

Halina Szatyłowicz*

Faculty of Chemistry, Warsaw University of Technology, Noakowskiego 3, 00-664 Warsaw, Poland

Tadeusz M. Krygowski

Department of Chemistry, Warsaw University, Pasteura 1, 02-093 Warsaw, Poland

Aneta Jezierska

Faculty of Chemistry, University of Wrocław, F. Joliot-Curie 14, 50-383 Wrocław Poland, and National Institute of Chemistry, Hajdrihova 19, 1001 Ljubljana, Slovenia

Jarosław J. Panek

Faculty of Chemistry, University of Wrocław, F. Joliot-Curie 14, 50-383 Wrocław, Poland

Received: December 11, 2008; Revised Manuscript Received: March 4, 2009

We were able to test the Bent−Walsh rule by examining geometric parameters in the vicinity of the *ipso*-carbon atom of H-bonded complexes of *para*-substituted phenol/phenolate and aniline/anilide derivatives for the three cases (i) *a* versus α, (ii) α versus d_{CO} or d_{CN}, and (iii) *a* versus d_{CO} or d_{CN}, where α is the ring valence angle at the *ipso*-carbon atom (C1 substituted by OH or O^- or NH_2 or NH^-) and *a* is the arithmetic mean of the two $C_{ipso}-C_{ortho}$ bond lengths. The data for nonequilibrium H-bonded complexes of unsubstituted phenol/phenolate and aniline/anilide with the respective bases F^- and CN^- and acids HF and HCN showed the same dependence of *a* on d_{CX} (X = O, N) as the data for equilibrium complexes of *para*-Y-substituted phenol/phenolate and aniline/anilide derivatives (Y = NO, NO_2, CHO, COMe, $CONH_2$, Cl, F, H, Me, OMe, OH) with the same bases and acids. The slope of these dependencies was negative, as expected. In the remaining cases (*a* versus α and α versus d_{CO} or d_{CN}), the slopes for simulated complexes followed the Bent−Walsh rule. Finally, for the equilibrium complexes in which the substituent effect was included, the slopes of the trend lines for the substituted systems were opposite. This is because in the *a* versus α relationships, electonegativity and the resonance effect act in the same direction, whereas for the other two cases, these effects are opposite, and the resonance effect dominates.

I. Introduction

Geometric parameters at the substituted carbon atom of monosubstituted benzene derivatives should follow the Bent−Walsh rule,[1] which says that "if a group X_1 attached to a carbon atom is replaced by a more electronegative group X_2, then the carbon atom's valency toward X_2 has a more p character than it had toward X_1".[1b] This, in turn, leads to a decrease in p character of the two other hybrid orbitals of the carbon atom and an increase in the α value (i.e., the bond angle of the aromatic ring at the *ipso*-carbon) and a shortening of the adjacent CC bond lengths, *a*. Thus, if we start from an idealized "pure sp^2" structure at the *ipso*-carbon atom in a substituted benzene, its sp^2-hybridized orbitals pointing toward the substituent become like $sp^{2+2\delta}$, whereas those directed toward C2 and C6 in the ring attain an $sp^{2-\delta}$ character (see Scheme 1). The Bent−Walsh rule is best explained in this context as a geometrical consequence of rehybridization occurring mainly at the *ipso*-carbon atom. Hybridization has for a long time been considered the principal factor affecting the shape and bonding pattern of organic molecules.[2] On the other hand, rehybridization can be explained on the basis of semiquantitative theories involving orbital overlaps[2b,c] or analyzed using a fully quantum chemical treatment.

SCHEME 1: Hybridization Trends at the *Ipso*-Carbon Atom Substituted by X_1 and X_2 Resulting from Changes in Their Electronegativity[a]

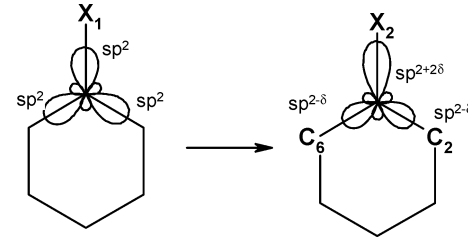

[a] X_2 is more electronegative than X_1. For clarity, an idealization of pure sp^2 hybridization in the presence of X_1 is assumed.

Domenicano et al. showed that[3] the experimentally determined changes in α, the bond angle at the C_{ipso}, correlate relatively well with the group electronegativity[4] as defined by Huheey,[5] which is in line with the Bent−Walsh rule. A recent

* To whom correspondence should be addressed. E-mail: halina@ch.pw.edu.pl. Phone: (+48) 22 2347755. Fax: (+48) 22 6282741.

10.1021/jp8109258 CCC: $40.75
Published on Web 04/15/2009

study by Domenicano et al.,[6] based on quantum chemical modeling of 74 monosubstituted benzene derivatives, showed that there is very good correlation between the *ipso* angle α and both $C_{ipso}-C_{ortho}$ bond lengths *a* provided that resonant substituents (strong π-donors and π-acceptors) are not taken into account. Moreover, they used the angular geometry of the monosubstituted benzene derivatives for estimating a new scale of group electronegativity.[7] By applying principal component analysis (PCA),[8] they showed that the main principal component, which explains most of the total variance, is dependent on the electronegativity of the substituent. However, the principal component second in importance was shown to be dependent on the resonance contribution of intramolecular interactions. Therefore, the question arises as to how the molecular properties change when the substituent is of the same kind in the whole series but its electronegativity changes. Following the theory by Iczkowski and Margrave,[9] it can be said that an increase in negative charge at the atomic moiety decreases its electronegativity. This situation was reported in the literature as a study of H-bonding effects on the geometry of the pentachlorophenol moiety in H-bonded complexes with various bases[10] since, as has been shown recently, the electronegativity of the hydroxyl group involved in H-bonding with bases changes its magnitude.[11] The most important result obtained by Wozniak et al.[10] was that the substituent effect (of the OH···base) on CC and CO bond lengths is mostly of the resonance type.

Another aspect of the substituent effect is related to the well-known dependence of changes in the magnitude of this effect on the type of reaction site. In this case, a nitro group serves as an excellent example.[12] Experimental[13] and theoretical studies[14] showed that the CN bond in nitrobenzene is almost exactly cylindrical, indicating a low contribution of the π character. This is in agreement with the conclusion resulting from a comparison of the Hammett substituent constant,[15] $\sigma_p = 0.78$, and the field effect, $\sigma_F = 0.65$. The magnitude of this effect increases substantially in systems with an electron-donating reaction site. For such systems, the substituent constant[15] is $\sigma_p^- = 1.27$, which shows that the substituent effect is very sensitive to the nature of the *para*-situated reaction site. It is clear that the potential electron-accepting power of the nitro group depends dramatically on whether the group may interact with the substituted moiety. A similar situation was found in other cases[16] in which the counterpart of the system, in our case, the region of H-bonding, is modified by the strength of the H-bond interactions.

The main aim of the present study is an investigation of how a mostly σ-electron effect of a substituent, such as the influence of a substituent's property, that is, its electronegativity, corresponds to the resonance effect, which is mostly associated with the π-electron structure.

II. Computational Methodology

The geometries of the investigated *para*-Y-substituted derivatives (where Y = NO, NO_2, CHO, COMe, $CONH_2$, Cl, F, H, Me, OMe, OH) of aniline and phenol and their H-bonded complexes with HB and B (where HB = HF and HCN, B = F^- and CN^-; for clarity, see Scheme 2) were obtained on the basis of density functional theory (DFT).[17] The three-parameter hybrid functional proposed by Becke[18] with a correlation energy according to the Lee−Yang−Parr formula,[19] denoted as B3LYP, was applied. The triple-ζ split-valence basis set with diffuse functions on non-hydrogen atoms and polarization functions on all atoms (d: non-hydrogen; p: hydrogen), denoted according to Pople's nomenclature as 6-311+G(d,p),[20] was used. The

SCHEME 2: Schematic Presentation of the Studied Complexes

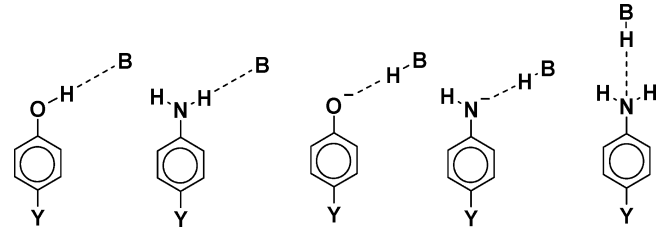

geometries of the H-bonded complexes were obtained, assuming linearity of the hydrogen bond, using two different strategies, (i) full geometry relaxation of all of the studied systems and (ii) simulation of the interaction between the components of complexes with a gradual change in its strength.

In the second case, the geometries of the complexes (Scheme 2, Y = H) were calculated from energy minimization for the fixed distances between the heavy atoms involved in the hydrogen bond (O···F or N···F and O···C or N···C) and optimization of the remaining internal degrees of freedom. First, the maximum distance between the heavy atoms involved in H-bond formation in the studied complexes (O···F, O···C, N···F, and N···C) was set to 4.0 Å. Then, it was shortened (using a 0.2 Å decrement) to (i) the distance corresponding to the minimum on the potential energy surface (PES) found by full geometry optimization or (ii) the distance at which proton transfer occurs.

At this point, it should be mentioned that the harmonic frequencies were calculated to confirm that the obtained geometry corresponded to a minimum on the potential energy surface (PES). In systems in which the hydrogen bond distance was longer than ∼3.0 (complexes with F^- or HF) or 3.4 Å (complexes with CN^- or HCN), the obtained structures had only one imaginary frequency, which indicates that the assumption of linearity of the intermolecular H-bond was correct. In addition, atomic charges according to the scheme proposed by Mulliken[21] were calculated. This part of the simulations was carried out using the Gaussian03[22] series of programs, which was subsequently used to generate wave functions for Atoms in Molecules (AIM) atomic charge calculations.[23,24] The AIM atomic charges were calculated by numerical integration of the electron density over the atomic domains provided by the level of DFT theory described above. The AIM analysis was performed using the AIMPAC package.[25]

III. Results and Discussion

As a result of the Bent−Walsh rule (see Introduction), three kinds of dependencies between bond lengths and bond angles should be observed, (i) *a* versus d_{CX}, (ii) *a* versus α, and (iii) α versus d_{CX}. However, it should be emphasized that in typical Bent−Walsh scatter plots, that is, for monosubstituted benzene derivatives,[6] it is not possible to observe the relationship between the C−X bond length and *a* or α precisely since the C−X interatomic distances depend dramatically on the nature and, particularly, the atomic radii of substituent X. These types of dependencies are possible for the systems presented in this paper since CX in our case is the CO or CN bond of H-bonded complexes in which these bonds are part of the H-bond region, as shown in Scheme 2. Hence, the properties of the CO and CN bonds depend on the strength of the H-bonding in question and may serve for construction of the scatter plots.

In the above cases, two factors are responsible for changes in the geometry of the systems, the substituent's (Y in the *para*

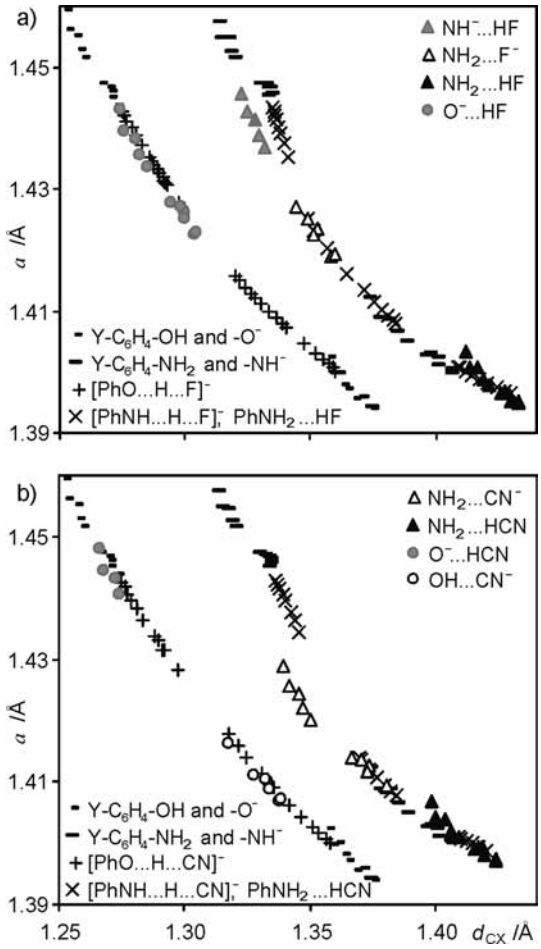

Figure 1. Dependencies of the mean value of the *a* bond length on the CN or CO bond lengths, d_{CX} (X = N, O), for *para*-Y-substituted phenol (short dashes) and aniline (long dashes) derivatives (Y = NO, NO_2, CHO, COMe, $CONH_2$, Cl, F, H, Me, OMe, OH) and their H-bonded complexes with B and HB (Scheme 2); (a) B = F^- and HB = HF, (b) B = CN^- and HB = HCN. Plus signs and crosses identify simulated H-bonded systems of phenol and aniline, respectively. Circles denote phenols and triangles aniline H-bonded equilibrium complexes; empty signs denote OH···B and NH_2···B interactions, gray signs denote O^-···HB and NH^-···HB interactions, and black signs denote NH_2···HB interactions.

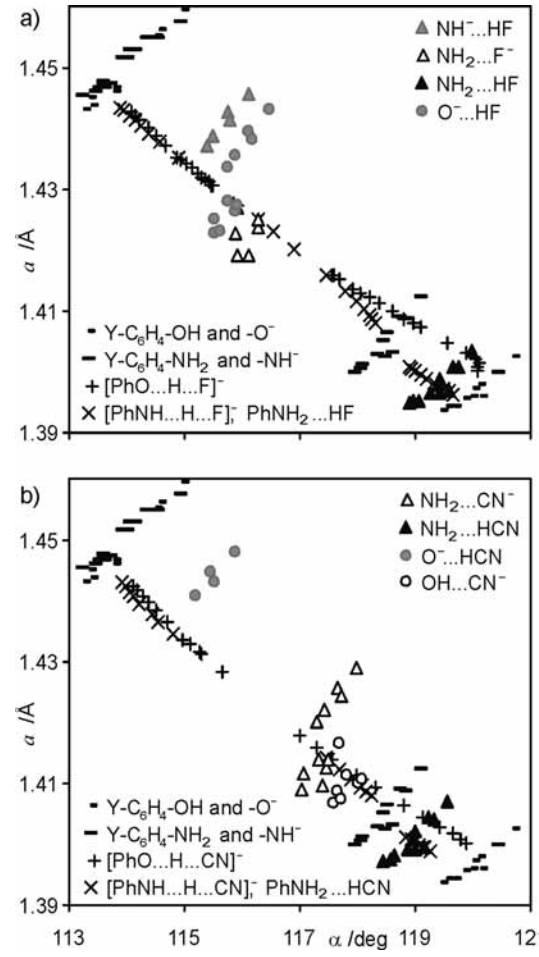

Figure 2. Dependencies of the mean value of the *a* bond length on the α angle for *para*-Y-substituted phenol (short dashes) and aniline (long dashes) derivatives (Y = NO, NO_2, CHO, COMe, $CONH_2$, Cl, F, H, Me, OMe, OH) and their H-bonded complexes with B and HB (Scheme 2); (a) B = F^- and HB = HF, (b) B = CN^- and HB = HCN. Plus signs and crosses identify simulated H-bonded systems of phenol and aniline, respectively. Circles denote phenols, and triangles denote aniline H-bonded equilibrium complexes; empty signs denote OH···B and NH_2···B interactions, gray signs denote O^-···HB and NH^-···HB interactions, and black signs denote NH_2···HB interactions.

position) effect on the hydrogen bond region and the changes in the H-bonding strength itself as a result of the approach of the partner in the intermolecular H-bond. Both of these factors modify the geometrical parameters of the α angle, *a*, and CN/CO bond lengths. The H-bonded systems presented in Scheme 2 can be understood as representations of two situations. One is an H-bonded equilibrium complex, and the other is a nonequilibrium situation in which the approach of the base B or acid HB to the other component of the hydrogen bond proceeds along the dotted line.

Figures 1, 2, and 4 present typical scatter plots of the investigation of the Bent−Walsh rule. To increase legibility, the H-bonded complexes of phenol and aniline derivatives have been divided into two subgroups. Their intermolecular interactions with HF or F^- (as BH or B, Scheme 2) are presented in part (a), and interactions with HCN or CN^- are shown in part (b) of the same figure. There are three cases of dependencies, (i) *a* versus d_{CX}, X = O, N, (ii) *a* versus α, and (iii) α versus d_{CX}. For the sake of clarity, they are considered separately.

Scatter Plots of *a* versus CN or CO Bond Lengths. Figure 1 shows two sets of data for hydrogen-bonded complexes as well as a set of uncomplexed (non-hydrogen-bonded) molecules with various substituents. The first set of hydrogen-bonded systems refers to the geometric patterns of equilibrium complexes as shown in the general view in Scheme 2. The second set of geometric data is taken from nonequilibrium complexes. This set is formed as follows.[26] The nitrogen atom or the NH group in the aniline/anilide derivatives or the oxygen atom or OH group of the phenolate/phenol derivatives is gradually approached by the acidic or basic moieties BH or B, respectively (in our case, HF, HCN or F^-, CN^-), as shown in Scheme 2. The strength of these nonequilibrium H-bonded complexes depends on the distance between the heavy-atom components of the H-bond; for aniline and anilide, this is $d_{N\cdots C}$ for interactions with HCN or CN^- and $d_{N\cdots F}$ for interactions with HF or F^-, whereas for phenol and phenolate, it is $d_{O\cdots F}$ for interactions with F^- or HF and $d_{O\cdots C}$ for interactions with HCN or CN^-. In all of these cases, the distances are controlled and gradually decreased from 4 Å down to the distance at which the equilibrium complex is formed. As shown in the scatter plot of Figure 1, the data for the equilibrium complexes (labeled in the right margin of the figure) lie on a line together with the nonequilibrium complexes (labeled in the left bottom margin

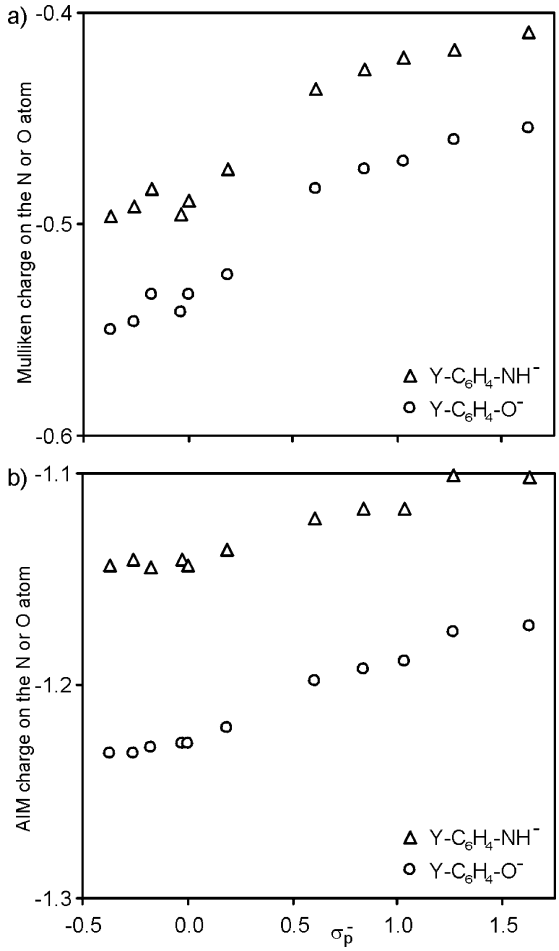

Figure 3. Dependence of (a) Mulliken and (b) AIM charges at the nitrogen atom in *para*-Y-substituted anilide and at the oxygen atom in *para*-Y-substituted phenolate derivatives on the σ_p^- constant.

of the figure), thereby supporting their use as a representation of the Bent−Walsh rule. The slightly greater dispersion of the data points for the aniline derivatives may result from the more complex interactions which take place in these cases than those in phenol and phenolate (Scheme 2).

Scatter Plot of *a* Bond Lengths versus α Bond Angles. The scatter plot presented in Figure 2 shows the geometric data for the H-bonded equilibrium complexes (labeled according to the legend in the right corner) and the nonequilibrium data (with labeling in the left bottom corner) for unsubstituted aniline, anilide, phenol, and phenolate systems to which, as mentioned above, the appropriate approach of the acidic or basic moieties (see Scheme 2) was applied. The graphs also include data for the uncomplexed (non-hydrogen-bonded) molecules differing in the *para* substituent.

As we can see in the scatter plot in Figure 2, the trend lines for *para*-substituted H-bonded equilibrium complexes are situated almost perpendicularly to the line which describes systems following the Bent−Walsh rule (denoted by + and × signs). The ranges of variation in the *a* bond lengths (∼1.39−∼1.46Å) and the bond angle (α ∼113−∼121 °) are substantial. The data in the subgroups containing *para*-substituted equilibrium H-bonded complexes of a particular type have much smaller ranges (0.01−0.02 Å in bond length and 1−2° in bond angle) but are still sufficient to be considered substantial deviations from typical Bent−Walsh plots. Moreover, for *para*-substituted anilide and phenolate derivatives and H-bonded complexes of type $O^-\cdots HF$, $O^-\cdots HCN$, $NH^-\cdots HF$, $NH^-\cdots HCN$, that is, when the "reaction site" is a H-bond region in which the H-donating system approaches the negatively charged proton acceptor, the dependencies of bond length *a* on angle α have positive slopes. For all of these cases, the most deviating points are for the nitroso substituent, that is, the most π-electron-accepting one. When the electron-accepting substituent is weaker, deviation from the Bent−Walsh line is smaller. It is a well-known observation that if there are substituents of opposite (donating versus accepting) electronic properties in the *para* positions of disubstituted benzene derivatives, the ring structure resembles a quinoid-like structure[27] and that the greater the sum of the absolute values of the respective substituent constants (σ^+ and σ^-), the greater the contribution of the quinoid-like structure in a given system.[28] Thus, in our case, the elongation of the *a* bonds is mostly due to the strong intramolecular charge transfer, which leads to the formation of a quinoid-like structure. The decrease in the electron-accepting power of the substituent leads to a diminished contribution of the quinoid structure and a smaller deviation of the data point from the Bent−Walsh line. However, a problem remains to be solved; why is the increase in electron-accepting power of the substituent associated with an increase in the bond angle at the *ipso*-carbon atom to which the O^-/NH^- moieties are attached? A possible explanation is that the charge transfer from O^- or NH^- toward the electron-accepting *para* substituent results in a decrease in electron charge at the oxygen and nitrogen atoms, respectively, thus causing an increase in their electronegativity.[11,29] This leads to an increase in the bond angle α. Figure 3, which presents the dependency of Mulliken[21] and AIM[23] atomic charges at the nitrogen and oxygen atoms in phenolate and anilide on the substituent constants, supports this view; the greater electron-accepting power (i.e., the greater the value of σ_p^-), the less negative the atoms in question.

The scatter plot is for the substituents NO, NO_2, CHO, $COCH_3$, $CONH_2$, Cl, F, H, CH_3, OCH_3, and OH, whereas σ_p^- is taken from a review article.[15] It is also shown in Figure 3 that for electron-donating substituents ($\sigma_p^- < 0$), the Mulliken charges at either the nitrogen or the oxygen atom do not depend so clearly on the substituent constants. The data points for these substituted systems subsequently behave more chaotically. The charges derived from AIM analysis of the electronic structure are more systematically ordered.

Plots of the α Angle versus CN or CO Bond Lengths. Scatter plots of the bond angle α versus d_{CN} or d_{CO} are presented in Figure 4. As in the dependencies discussed above, the data for variously substituted and isolated molecules are included together with the hydrogen-bonded complexes. Similar to the former case, we observe deviations of the data points for the equilibrium H-bonded complexes for *para*-substituted systems from the trends for the non-equilibrium complexes of the unsubstituted phenol/phenolate and aniline/anilide systems. This similarity to α angle versus *a* bond length plots (see Figure 2) is again due to the fact that one variable, the bond angle α, depends mostly on the electronegativity of the substituent at the *ipso* position, whereas the other variable, d_{CN} or d_{CO}, depends mostly on the resonance effect, thus, on the nature of the *para* substituent interacting with the group forming the H-bond. Thus, for nonequilibrium complexes of unsubstituted H-bonded phenol/phenolate and aniline/anilide, we have an almost "purely" electronegativity-borne effect. This is not the case for *para*-substituted equilibrium H-bonded complexes in which, apart from the effect of electronegativity (and its changes due to the variations of charge at the oxygen

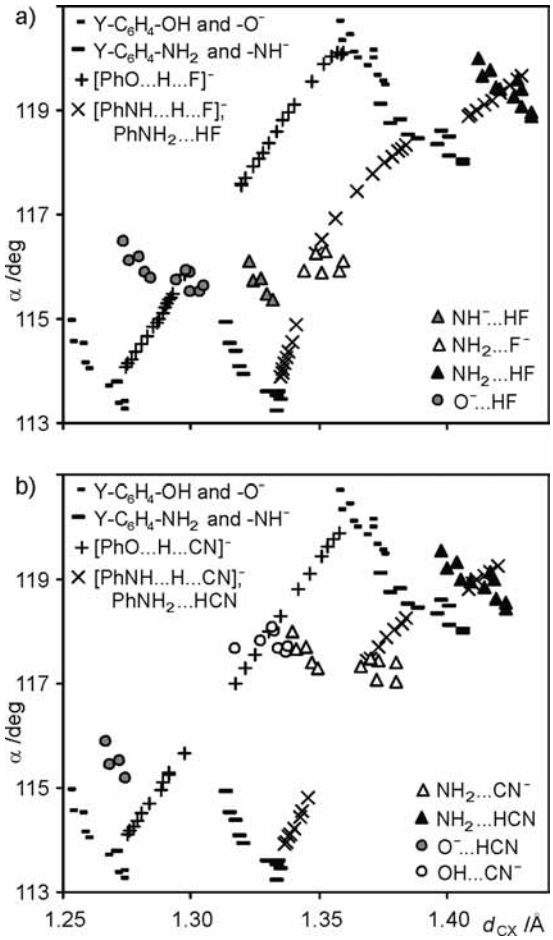

Figure 4. Dependencies of α angle on CN or CO bond lengths, d_{CX} (X = N, O), for *para*-Y-substituted phenol (short dashes) and aniline (long dashes) derivatives (Y = NO, NO_2, CHO, COMe, $CONH_2$, Cl, F, H, Me, OMe, OH) and their H-bonded complexes with B and HB (Scheme 2); (a) B = F^- and HB = HF, (b) B = CN^- and HB = HCN. Plus signs and crosses identify simulated H-bonded systems of phenol and aniline, respectively. Circles denote phenols and triangles aniline H-bonded equilibrium complexes; empty signs denote OH···B and NH_2···B interactions, gray signs denote O^-···HB and NH^-···HB interactions, and black signs denote NH_2···HB interactions.

or nitrogen atoms), a strong resonance effect appears, leading to the quinoid-like structure, which is also associated with a decrease in charge at the N or O atoms and in turn an increase in their electronegativity.

IV. Conclusions

This study presents, for the first time, a complete set of consequences related to the Bent−Walsh rule for three types of dependences, *a* versus α, α versus d_{CO} or d_{CN}, and *a* versus d_{CO} or d_{CN}. Previously published reports included only mono-substituted systems and presented only dependences of the "*a* versus α" type. Here, we showed that the rule also works well for unsubstituted systems in which the electronegativity of the group involved in the H-bonding is decisive. In the cases of *para*-substituted derivatives, particularly with groups of electron-attracting properties, it seems that the rule does not work due to intramolecular charge transfer from the H-bond region to the *para* substituent. Only in the case of the relationship between *a* bond lengths and d_{CN} for *para*-substituted aniline/anilide or d_{CO} for phenol/phenolate is the dependence consistently monotonic. This is because in these cases, the magnitudes of d_{CO} and d_{CN} as well as that of the *a* bond lengths depend mostly on the same type of interaction, intramolecular charge transfer leading to a quinoid-like structure.

Acknowledgment. This paper is dedicated to Prof. Christian Reichardt (Marburg, Germany) on the occasion of his 75th birthday. H.S. and T.M.K. thank the Interdisciplinary Center for Mathematical and Computational Modeling (Warsaw, Poland) for computational facilities, and H.S. thanks the Warsaw University of Technology for financial support. In addition, A.J. and J.J.P. gratefully acknowledge the Wrocław Center for Networking and Supercomputing (WCSS) and the Poznań Supercomputing and Networking Center for providing computer time and facilities.

References and Notes

(1) (a) Walsh, A. D. *Discuss. Faraday Soc.* **1947**, *2*, 18–25. (b) Bent, H. A. *Chem. Rev.* **1961**, *61*, 275–311.
(2) (a) Kovaèevic, K.; Maksic, Z. B. *J. Org. Chem.* **1974**, *39*, 539–545. (b) Maksic, Z. B.; Rubèic, A. *J. Am. Chem. Soc.* **1977**, *99*, 4233–4241. (c) Maksic, Z. B. *Comput. Math. Appl.* **1986**, *12*, 697–723.
(3) (a) Domenicano, A.; Vaciago, A.; Coulson, C. A. *Acta Crystallogr.* **1975**, *B31*, 221–234. (b) Domenicano, A.; Vaciago, A.; Coulson, C. A. *Acta Crystallogr.* **1975**, *B31*, 1630–1641. (c) Domenicano, A.; Murray-Rust, P. *Tetrahedron Lett.* **1979**, *20*, 2283–2296. (d) Domenicano, A.; Murray-Rust, P.; Vaciago, A. *Acta Crystallogr.* **1983**, *B39*, 457–468.
(4) Korchowiec, J.; Nalewajski, R. F. *Int. J. Quantum Chem.* **1992**, *44*, 1027–1040.
(5) (a) Huheey, J. *Phys. Chem.* **1965**, *69*, 3284–3291. (b) Huheey, J. *J. Phys. Chem.* **1966**, *70*, 2086–2092.
(6) Campanelli, A. R.; Domenicano, A.; Ramondo, F. *J. Phys. Chem. A* **2003**, *107*, 6429–6440.
(7) Campanelli, A. R.; Domenicano, A.; Ramondo, F.; Hargittai, I. *J. Phys. Chem. A* **2004**, *108*, 4940–4948.
(8) Zalewski, R. I. In *Similarity Models in Organic Chemistry, Biochemistry and Related Fields*; Zalewski, R. I., Krygowski, T. M., Shorter, J., Eds.; Elsevier: Amsterdam, The Netherlands, 1991; Chapter 9, p 453.
(9) Iczkowski, R. P.; Margrave, J. L. *J. Am. Chem. Soc.* **1961**, *83*, 3547–3551.
(10) Woźniak, K.; Krygowski, T. M.; Kariuki, B.; Jones, W. *J. Mol. Struct.* **1991**, *248*, 331–343.
(11) Krygowski, T. M.; Szatyłowicz, H. *J. Phys. Chem. A* **2006**, *110*, 7232–7236.
(12) Exner, O.; Krygowski, T. M. *Chem. Soc. Rev.* **1996**, *25*, 71–75.
(13) Boese, R.; Blaser, D.; Krygowski, T. M. *Struct. Chem.* **1992**, *3*, 363–368.
(14) Irle, S.; Krygowski, T. M.; Niu, J. E.; Schwarz, W. H. E. *J. Org. Chem.* **1995**, *60*, 6744–6755.
(15) Hansch, C.; Leo, A.; Taft, R. W. *Chem. Rev.* **1991**, *91*, 165–195.
(16) (a) Szatyłowicz, H.; Krygowski, T. M.; Zachara-Horeglad, J. E. *J. Chem. Inf. Model.* **2007**, *47*, 875–886. (b) Krygowski, T. M.; Szatyłowicz, H. *Trends Org. Chem.* **2006**, *11*, 37–53.
(17) (a) Hohenberg, P.; Kohn, W. *Phys. Rev.* **1964**, *136*, B864−B871. (b) Kohn, W.; Sham, L. J. *Phys. Rev.* **1965**, *140*, A1133−A1138. (c) Stephens, P. J.; Devlin, F. J.; Chabalowski, C. F.; Frisch, M. J. *J. Phys. Chem.* **1994**, *98*, 11623–11627.
(18) (a) Becke, A. D. *J. Chem. Phys.* **1993**, *98*, 1372–1377. (b) Becke, A. D. *J. Chem. Phys.* **1993**, *98*, 5648–5652.
(19) Lee, C.; Yang, W.; Parr, R G. *Phys. Rev. B* **1988**, *37*, 785–789.
(20) Krishnan, R.; Binkley, J. S.; Seeger, R.; Pople, J. A. *J. Chem. Phys.* **1980**, *72*, 650–654.
(21) Mulliken, R. S. *J. Chem. Phys.* **1955**, *23*, 1833–1840.
(22) Frisch, M. J.; Trucks, G. W.; Schlegel, H. B.; Scuseria, G. E.; Robb, M. A.; Cheeseman, J. R.; Montgomery, J. A., Jr.; Vreven, T.; Kudin, K. N.; Burant, J. C.; Millam, J. M.; Iyengar, S. S.; Tomasi, J.; Barone, V.; Mennucci, B.; Cossi, M.; Scalmani, G.; Rega, N.; Petersson, G. A.; Nakatsuji, H.; Hada, M.; Ehara, M.; Toyota, K.; Fukuda, R.; Hasegawa, J.; Ishida, M.; Nakajima, T.; Honda, Y.; Kitao, O.; Nakai, H.; Klene, M.; Li, X.; Knox, J. E.; Hratchian, H. P.; Cross, J. B.; Bakken, V.; Adamo, C.; Jaramillo, J.; Gomperts, R.; Stratmann, R. E.; Yazyev, O.; Austin, A. J.; Cammi, R.; Pomelli, C.; Ochterski, J. W.; Ayala, P. Y.; Morokuma, K.; Voth, G. A.; Salvador, P.; Dannenberg, J. J.; Zakrzewski, V. G.; Dapprich, S.; Daniels, A. D.; Strain, M. C.; Farkas, O.; Malick, D. K.; Rabuck, A. D.; Raghavachari, K.; Foresman, J. B.; Ortiz, J. V.; Cui, Q.; Baboul, A. G.; Clifford, S.; Cioslowski, J.; Stefanov, B. B.; Liu, G.; Liashenko, A.; Piskorz, P.; Komaromi, I.; Martin, R. L.; Fox, D. J.; Keith, T.; Al-Laham, M. A.; Peng, C. Y.; Nanayakkara, A.; Challacombe, M.; Gill, P. M. W.; Johnson, B.; Chen, W.; Wong, M. W.; Gonzalez, C.; Pople, J. A. *Gaussian 03*, revision A.1; Gaussian, Inc.: Pittsburgh, PA, 2004.

(23) Bader, R. F. W. *Atoms in Molecules, A Quantum Theory*; Clarendon Press: Oxford U.K., 1990.
(24) Bader, R. F. W.; Beddall, P. M. *J. Chem. Phys.* **1972**, *56*, 3320.
(25) Bader, R. F. W. *AIMPAC, Suite of programs for the Theory of Atoms in Molecules*; McMaster University: Hamilton, Ontario, Canada, 1991.
(26) For details see: Krygowski, T. M.; Zachara, J. E.; Szatyłowicz, H. *J. Phys. Org. Chem.* **2005**, *18*, 110–114.
(27) (a) Hiberty, P. C.; Ohanessian, G. *J. Am. Chem. Soc.* **1984**, *106*, 6963–6968. (b) Krygowski, T. M.; Maurin, J. *J. Chem. Soc., Perkin Trans. 2* **1989**, 695–698.
(28) Krygowski, T. M. *J. Chem. Res.* **1987**, 120–121.
(29) Szatyłowicz, H.; Krygowski, T. M. *J. Mol. Struct.* **2007**, *844/845*, 200–207.

JP8109258